

~~SECRET~~

D

BIF-107-25012-69  
Copy No. 1 of 2  
Pages: 13

TO: A. D. Halenbeck

DATE: 25 April 1969

SUBJECT: Current Ephemeris Error Estimates  
And Related Discussion

FROM: L. J. Tedeschi

---

Estimates of MOL ephemeris errors if MOL were operational today (April 1969) have been inferred from 18 Program 110 and 4 Program 206 flight histories. These records, comprised of orbit fitting and prediction performance, drag estimates, magnetic activity indices, orbit adjusts, etc., are documented in the Preliminary Flight Evaluation Reports (Reference 1).

The selection of Programs 110 and 206 prediction performance for MOL prediction estimates was considered reasonable because of the similarity of orbits and ballistic coefficients. Drag and gravitational perturbations, which are the dominant factors affecting orbit navigation performance, would then be essentially equivalent for the two vehicles if flown today. The dominant perturbation affecting prediction over a few revs or more is drag. For shorter prediction intervals of 1-3 revs, errors in estimating the initial state, and errors in the gravity field are very significant in addition to drag. An attempt has been made to separate out these three factors for Program 110. The method, outlined in Reference 2, has been applied by Aerospace Program 110 personnel at the STC to 9 of the aforementioned 18 flights. Their results have been considered in the error breakdowns estimated for MOL.

Based on flight experience it has been found that drag effects are highly variable depending on the dynamic state of the atmosphere. A positive correlation has been observed between prediction performance and an index known as  $A_p$ , the "planetary" solar magnetic activity index. Unfortunately,  $A_p$  values (averaged from 12 stations over the globe) are only obtainable some time after the occurrence of the activity and therefore cannot be used. Instead, certain local measures, designated as  $A_k$ , are utilized. These index values are collected by the Air Force Air Weather Service from stations at Fredericksburg, Virginia; Thule, Greenland; Loring Air Force Base, Maine; and College, Alaska. They are made available on a real time basis at three-hour intervals. The  $A_k$  numbers are used to establish levels of solar activity and consequent atmospheric disturbances.

Operational prediction results are summarized in Figure 1, whose ordinate shows the RMS in-track prediction errors in hundreds of feet, and the abscissa indexes the revs past epoch in the prediction interval. Present operational data fitting procedures place the epoch vector immediately following the last station pass of a fit.

~~SECRET~~

D

HANDLE VIA BYEMAN  
CONTROL SYSTEM ONLY

~~SECRET~~ D

Bif-107-25012-69

Page 2

The bands labelled "low", "moderate", and "high" indicate the degree of solar magnetic activity associated with a particular in-track error level. The outer boundaries of the error swath were merely the lowest and highest RMS values realized in the 22 flights analyzed. The intermediate boundaries were determined by noting the history of reported  $A_k$  values slightly before and during the time interval of prediction sets yielding a particular RMS in-track error. These intermediate boundaries are necessarily not precise because of the difficulty in obtaining a rigorous quantitative correlation between in-track error and  $A_k$  history. In this respect it is noted that some flights appeared at more than one error level on the plot according to the different degrees of solar activity experienced during a flight. The subdivisions of such flights were taken no shorter than 2-3 days and contained predictions from about thirty 12-rev fits.

The prediction errors shown in Figure 1 are seen to increase with length of prediction interval and degree of solar activity. In terms of data distribution within each band, the 34 points from 22 flights (including sub-spans) were distributed as follows: two in the low activity band, 21 in the moderate band, and 11 in the high band, with the "center of gravity" of the points about sixty percent of the geometric, not ordinate, distance, up the error swath from the lower boundary.

A breakdown of in-track prediction error causes is illustrated schematically in Figure 2. A 12-rev, split B fit (see Appendix), with epoch at the end of the fit produces in-track errors in the predict interval of three types. The first (labelled I. C. error) is the result of an in-track error at epoch plus the propagated effect of geopotential errors. This I. C. error propagates with negligible secular growth, and so is shown as a horizontal line. The second (labelled PERIOD error) increases linearly due to a period error in the epoch vector. This faulty period is believed to be mainly due to the use of incorrect drag during the fit interval. Note that I. C. error and PERIOD error cannot be compensated for by the use of an on-board update algorithm using accelerometer data in the predict interval. The third type (labelled PREDICT DRAG error) grows quadratically, and is due to the use of incorrect drag in the predict interval. It is this portion only which can be significantly reduced by the use of an on-board update algorithm using accelerometer data.

At the lower right of Figure 1 are presented the RMS errors in the radial and cross-track directions. The basis for these numbers is a post-flight analysis involving 16 command vectors from two flights, and best fit ephemerides (BFE's) used as references in the appropriate prediction intervals. The RMS radial and cross-track prediction errors originally obtained from detailed ephemeris difference runs were 225 ft. and 255 ft., respectively, at the mid latitude region of the northern hemisphere for a southbound satellite. To check the dispersion in the reference values, four sliding BFE's were then differenced over a common time interval, and the RMS radial position variation at mid-latitude for ten common revs was 550 ft., and the corresponding cross-track value was 400 ft. In view of the much higher values of reference dispersion as compared to the originally reported errors, it was decided to state the RMS radial and cross-track prediction errors as 500 ft., which are within specifications.

~~SECRET~~ D

~~SECRET~~

The MOL design point of 1800 ft. ( $2\sigma$ ) in-track prediction error at 2 1/2 revs past epoch will now be considered relative to Figure 1. At 2 1/2 revs past epoch, the ordinate location in terms of what is now most likely to be achieved, is at the "center of gravity" of the chart's data points (previously mentioned), or about 60 percent of the geometric, not ordinate, distance up the error swath from the lower boundary. This point is shown by an asterisk in Figure 1, and the RMS ( $\sim 1\sigma$ ) in-track prediction error there is 4000 ft., or a  $2\sigma$  value of 8000 ft., far higher than the 1800 ft. of the specifications. A numerical breakdown of error causes for this error level and prediction interval (4000 ft. at 2 1/2 revs past epoch) was carried out using operational data. From 35 12-rev fits, RMS values were obtained for the I.C., PERIOD, and DRAG contributions to the total in-track error. On a variance ( $2\sigma$ ) basis, the percentage of each contribution to the total error was as follows, rounding off for purposes of discussion:

|        |   |     |
|--------|---|-----|
| I.C.   | ≈ | 10% |
| PERIOD | ≈ | 65% |
| DRAG   | ≈ | 25% |

In terms of  $2\sigma$  values in feet, the contributions are as follows:

|        |   |      |
|--------|---|------|
| I.C.   | ~ | 2500 |
| PERIOD | ~ | 6500 |
| DRAG   | ~ | 4000 |

Note that the in-track errors due to I.C. and PERIOD errors are above (i. e., do not meet) the MOL specification. In addition, the reader is reminded that the on-board update algorithm using accelerometer data cannot make up for these errors (only DRAG errors). However, the use of accelerometer data in the fitting interval is expected to substantially reduce the I.C. and PERIOD errors to acceptable levels. The general applicability of Figure 1 to the MOL vehicle and orbit is indicated by the range of conditions shown at the upper left of the figure, and the amount of operational data involved should provide a basis for confidence in the numbers obtained from the chart. Construction of the chart from available data is explained in the Appendix

#### Discussion of Error Sources

The largest error source in the present state-of-the-art of orbit determination and prediction is the atmosphere model. Deficiencies in the model cause errors in drag determination in both the fit and predict intervals with consequently high prediction errors. The contribution to prediction errors by drag errors within the fit interval is more difficult to assess than that due to drag errors in the prediction interval. In this document, the former are included in the I.C. and PERIOD errors while the latter are called DRAG errors. Some near-term improvements in atmosphere modelling are possible; another approach to the drag problem is to employ a low-g accelerometer, already mentioned, and incorporate its drag measurement data into the orbit ephemeris program. This is discussed in the next section.

~~SECRET~~

~~SECRET~~

D

The next largest error source (other than vehicle originated forces) is the geopotential model. Studies have shown that this source may contribute from 400-1600 ft. ( $2\sigma$ ) to the in-track error, the number depending on length and location of fit span, and sophistication of the model. A firm determination of geopotential effects for low altitude satellites is made difficult by the dominance of atmospheric drag which tends to mask these effects. They can be inferred, however, from high-altitude, or essentially drag-free, satellites. A family of such satellites which has made the most reliable assessment of geopotential error effects has been the TRANSIT series. These satellites have flown at altitudes of 500-600 n mi, which are, of course, much higher than the MOL operational altitudes. Since gravity field effects become stronger with decreasing altitude, the TRANSIT results had to be adjusted for application at MOL altitudes. An estimate for the ratio of ephemeris errors due to geopotential errors in going from TRANSIT altitudes to MOL altitudes is about 3 to 1, this ratio having been deduced from simulation runs at Aerospace, and is also based on information cited in References 3 and 4. The lower bound of in-track errors due to geopotential errors (400 ft.) was determined by applying the 3 to 1 ratio to an optimistic estimate of 66 ft. ( $1\sigma$ ) for satellites of the TRANSIT class, including GEOS 1. This number is representative of the best possible performance cited in Reference 7, and corroborated by Reference 4. The upper bound of ephemeris error due to gravity field error was determined from an Aerospace simulation (Reference 8) which computed RMS ephemeris differences of 800 ft. at 80 n mi perigee due to fitting with the NWL 5E model (seventh degree) and the APL eighth degree models. Also, RMS ephemeris differences between the SAO 1966 model and the APL eighth degree model were computed at about 630 ft. at 165 n mi perigee in more recent tests. There is more hope for improvement in such models than is the case for the atmosphere, especially if a low-g accelerometer can be used to replace the drag model, and allow better determination of the geopotential field for MOL.

The contribution to in-track error from tracking station location errors is about the same magnitude as these errors. For the present SCF net, station location errors are on the order of 100-150 ft. ( $1\sigma$ ), but subsequent improvements are expected to reduce these errors to about 50 ft. ( $1\sigma$ ) by tying into the Navy TRANSIT Tracking Net (conservative estimate based on Reference 6).

The noise and bias characteristics of the SGLS data to be used subsequently are not expected to be significant sources of in-track error. The software computation and on-board ephemeris interpolation errors are expected to contribute even less significantly to the total in-track error.

#### Reduction of Ephemeris Errors

Three methods for reducing ephemeris errors will be discussed in this section, and they are the following:

1. Low-g accelerometer (LGA)
2. Last radar look (LRL)
3. Position learning

~~SECRET~~

D

~~SECRET~~ D

The LGA data can be used as a drag model replacement when fitting data and also in the predict interval either as a drag replacement, or for correcting the drag values generated by the software. The LRL provides a timing correction based on the difference between the predicted and actual time of arrival of a satellite over a tracking station. As such, this technique can reduce in-track errors which are not due to drag in the predict interval, and cannot be corrected by the LGA. A prime example of this non-drag contribution is that due to period error at epoch.

Table 1 lists representative values of prediction ephemeris error reduction through LGA and LRL. The top line of the table contains the "current" point of 8000 ft. ( $2\sigma$ ) in-track error at 2 1/2 revs obtained from Figure 1. This has been broken down, through the analysis of operational data mentioned previously, into component contributions from period error at epoch (PERIOD), drag error in prediction interval (DRAG), and initial condition error in position (I. C.).

The second line of Table 1 shows the effect of incorporating the LGA in the data fitting process. Reduction of the PERIOD error and I. C. is realized through the overcoming of atmosphere model deficiencies by the LGA, thus improving the fit and resulting epoch vector. The extent of this improvement may be inferred by prediction performance of the aforementioned TRANSIT satellites (essentially drag-free). Reference 5 contains plots of TRANSIT prediction performance indicating no secular in-track error growth for one day after fitting; i. e., there is no PERIOD error contribution. In Table 1, however, a non-zero value of 500 ft. is entered under PERIOD on the second line to account for LGA instrument errors and other uncertainties. This figure is admittedly not as well-founded as those on the first line, but because of the lack of supporting data, the number is presented on a "best judgement" basis. Improvement of the fit and epoch vector also reduces the I. C. error contribution, and the remaining 400-1600 ft. shown on the second line of Table 1 reflect the short-period geopotential effects which are not compensated by the LGA. These depend on fit and epoch vector locations, and the numbers quoted range from the most optimistic to the most pessimistic estimates, as discussed in the previous section. The DRAG contribution to the in-track error remains at 4000 ft. on the second line since the LGA is not used in the predict interval, and the environment in this interval is essentially uncorrelated to that of the fit interval.

The error reduction through use of the LGA in the predict interval is shown on the third line of Table 1. This improvement is in the DRAG contribution since the LGA senses the actual drag experienced in the interval as compared to that computed by the software. The 500 ft. shown under DRAG on the third line is due to errors in the LGA instrument and in the on-board algorithm computations. The I. C. contribution on this line is unchanged from the previous case since it is due to geopotential effects, not measured by the LGA.

Before closing the discussion of LGA application, it is noted that forthcoming flights of the instrument on an experimental basis will likely result in some improvement of the atmosphere model. Consequent reduction in "current" prediction error levels (line 1) may be expected, but it is not anticipated that the MOL prediction error specifications will be met by atmosphere model improvement alone.

~~SECRET~~ D

~~SECRET~~

BIF-107-25012-69

Page 6

The fourth and fifth lines of Figure 3 show the improvement to be gained through the use of LRL. Numbers tabulated are 2 1/2 rev predictions when the LRL corrections are applied at the revs indicated. The effect of this technique is to translate an error propagation curve towards the abscissa, thus reducing both the PERIOD and DRAG error contributions. The degree of error reduction increases as the point of LRL correction moves closer to the point of prediction (line 5 compared to line 4).

Lines 6 and 7 of Figure 3 display results of extrapolating an LRL reading by passing a straight line through the correction value at the reading and an assumed zero error at epoch. This extrapolation technique is a step better than the single point correction since the latter simply corrects the in-track error at one point but retains the propagation rates of the PERIOD and DRAG errors. By extrapolating the correction on a straight line basis, the PERIOD error propagation (linear) is essentially compensated. If the I.C. contribution were zero, as assumed in the extrapolation, the PERIOD error propagation would be exactly compensated but since this is not the case, entries at approximately zero are shown under the PERIOD column in lines 6 and 7.

The I.C. error contributions in Table 1 do not show a reduction through application of LRL. As mentioned previously, these components are due to short-period (orbital frequency) geopotential effects, and their reduction depends on knowledge of the relative positions of LRL and point of prediction on this periodic error curve. At present, it is not possible to determine this relationship on a real time basis (only by post-flight analysis). However, it may be possible to develop techniques which relate the LRL information to data within a fit (station time biases, for example) such that a reduction in geopotential error contribution may be realized through LRL. This possibility, the error reductions already shown, and the "backup" function the LRL would provide against possible LGA malfunction, are factors in favor of incorporating this capability on the MOL vehicle.

The last two lines of Table 1 indicate what may be achieved through an improvement of the geopotential model; that is, the I.C. error contributions are now at the lowest, or objective, values. Any improvement in this area, however, should be weighed against increased complexity of the model and consequent reduction of computational speed.

Table 2 presents data similar to that of Table 1, but at 2 revs downstream in the prediction interval, or 4 1/2 revs past epoch. The initial  $2\sigma$  in-track error of 18000 ft. was obtained from Figure 1 (asterisk at  $1\sigma = 9000$  ft.), and broken down into component contributions as before. It is seen that at this prediction interval the PERIOD and DRAG error contributions are equal and that the I.C. contribution is comparatively small. The entries under PERIOD for the LGA in fit (lines 2 and 3) were increased linearly over those of Table 1 because of the added 2 revs of predict. The entry under DRAG for LGA in predict (line 3) was also increased, but quadratically, over that of Table 1 because of the extended prediction interval. Though some numbers such as these may differ from one table to the other, the discussion accompanying Table 1 is also applicable to Table 2, as are the conclusions.

~~SECRET~~

~~SECRET~~ D

BIF-107-25012-69

Page 7

The technique of position learning has been applied in two cases of measurements at two initial ephemeris uncertainty levels. The analysis assumed crew angular measurements to a landmark using the ATS, and the two cases at each error level were for a single pair of measurements (obliquity and stereo angles, one sighting), and four pairs of measurements. The two ephemeris uncertainty levels reflected the present operational capability ( $2\sigma$  in-track error of 8000 ft. at 2 1/2 revs past epoch), and the MOL specification requirements ( $2\sigma$  in-track error 1800 ft. at 2 1/2 revs past epoch).

Realistic models of measurement noise ( $2\sigma = .250$  minutes of arc about each axis of the ATS) were used, and the data taken were optimally processed with a Kalman filter. Studies have indicated, however, that near-optimum results can be achieved with simplified sub-optimal methods. Fifteen scalar error sources were also used in the analysis, and these included satellite position and velocity errors, landmark position errors, and attitude, attitude rate errors. Some of these errors, on a  $2\sigma$  basis, were as follows:

|                       |  |
|-----------------------|--|
| Landmark location     | 1500 ft. in lat. , long<br>500 ft. in alt. |
| Vehicle attitude      | 6 min. of arc about each axis              |
| Vehicle attitude rate | 6 deg. /hr. about each axis                |

Results of the analysis showed that for an initial  $2\sigma$  in-track ephemeris error of 8000 ft. , a single pair of angular measurements reduced the uncertainty to 1900 ft. ( $2\sigma$ ), while four pairs of measurements reduced the uncertainty to 1500 ft. ( $2\sigma$ ). Equivalent reductions from an initial ephemeris error of 1800 ft. ( $2\sigma$ ) were to 1300 ft. and 1200 ft. , both  $2\sigma$  numbers. Covariance matrices were used to obtain the above values.

The foregoing data were furnished by H. T. Hendrickson, and further details of the analysis will be described in a forthcoming document.

L. J. Tedeschi  
L. J. Tedeschi

LJT/jaw

Attachments: Tables 1 and 2  
Figures 1 and 2  
Appendix (1page)

~~SECRET~~

~~SECRET~~

REFERENCES

1. Preliminary Flight Evaluation Reports. These are available from the 110 Program Office. (SECRET)
2. "Orbit Determination and Prediction Analysis Using a Simplified Method" (U), Aerospace ATM-68(3110-01)-49, by L. J. Tedeschi, 11 October 1967. (CONFIDENTIAL)
3. "Amplitude Spectra of the Low Degree Anomalous Gravity Field", Aerospace ATM 67-(2352)-7, by L. Wong, 5 December 1966
4. "Aliasing Effect of Neglected Gravity Coefficients on Accuracy of Orbit Computation", NWL Technical Report TR-2242, by H. L. Green, Jr., January 1969
5. "Error Analysis of the Navy Doppler Tracking System Applied to Geodetic Operations", NWL Technical Memorandum No. K-14/65, by R. J. Anderle, January 1965 (UNCLASSIFIED)
6. "NWL 8D Geodetic Parameters Based on Doppler Satellite Observations", NWL Technical Report No. 2106, by R. J. Anderle and S. J. Smith, July 1967
7. "Geodetic Satellite Results During 1967", Smithsonian Astrophysical Observatory Special Report No. 264, edited by C. A. Lundquist, 29 December 1967
8. "Anticipated Effects of Solar Cycle Peak and Perigee Altitude", Aerospace ATM 66(6119)-1, by R. W. Bruce, R. J. Farrar and C. M. Price, 22 March 1966

~~SECRET~~



~~CONFIDENTIAL~~

TABLE 1

ANALYSIS OF IN-TRACK ERROR REDUCTION  
AT 2 1/2 REVS PAST EPOCH USING  
REPRESENTATIVE VALUES

$$2\sigma \Delta \text{In-Track} = \sqrt{(2\sigma)_{\text{Per}}^2 + (2\sigma)_{\text{Drag}}^2 + (2\sigma)_{\text{IC}}^2}$$

$$\left[ \begin{array}{l} 1800 \text{ Ft Spec} \\ 600 \text{ Ft Obj} \end{array} \right]$$

|  | <u>Total</u> | <u>Period</u> | <u>Drag</u> | <u>IC</u>       |
|--|--------------|---------------|-------------|-----------------|
| W/O LGA/LRL<br>In Fit or Predict         | 8000         | 6500          | 4000        | 2500            |
| W LGA In Fit                             | 4050 - 4340  | 500           | 4000        | 400 - 1600      |
| W LGA In Fit<br>and Predict              | 800 - 1750   | 500           | 500         | 400 - 1600      |
| Above Plus Single LRL At                 |              |               |             |                 |
| E + 1                                    | 650 - 1700   | 300           | 400         | 400 - 1600      |
| E + 2                                    | 450 - 1600   | 100           | 200         | 400 - 1600      |
| Above Plus LRL<br>Extrapolation at E and |              |               |             |                 |
| E + 1                                    | 550 - 1650   | ≈ 0           | 400         | 400 - 1600      |
| E + 2                                    | 450 - 1600   | ≈ 0           | 200         | 400 - 1600      |
| Above Plus Geopotential<br>Improvement   |              |               |             |                 |
| E + 1                                    | 550          | ≈ 0           | 400         | 400 } Objective |
| E + 2                                    | 450          | ≈ 0           | 200         | 400 }           |

~~CONFIDENTIAL~~

~~SECRET~~ D

TABLE 2

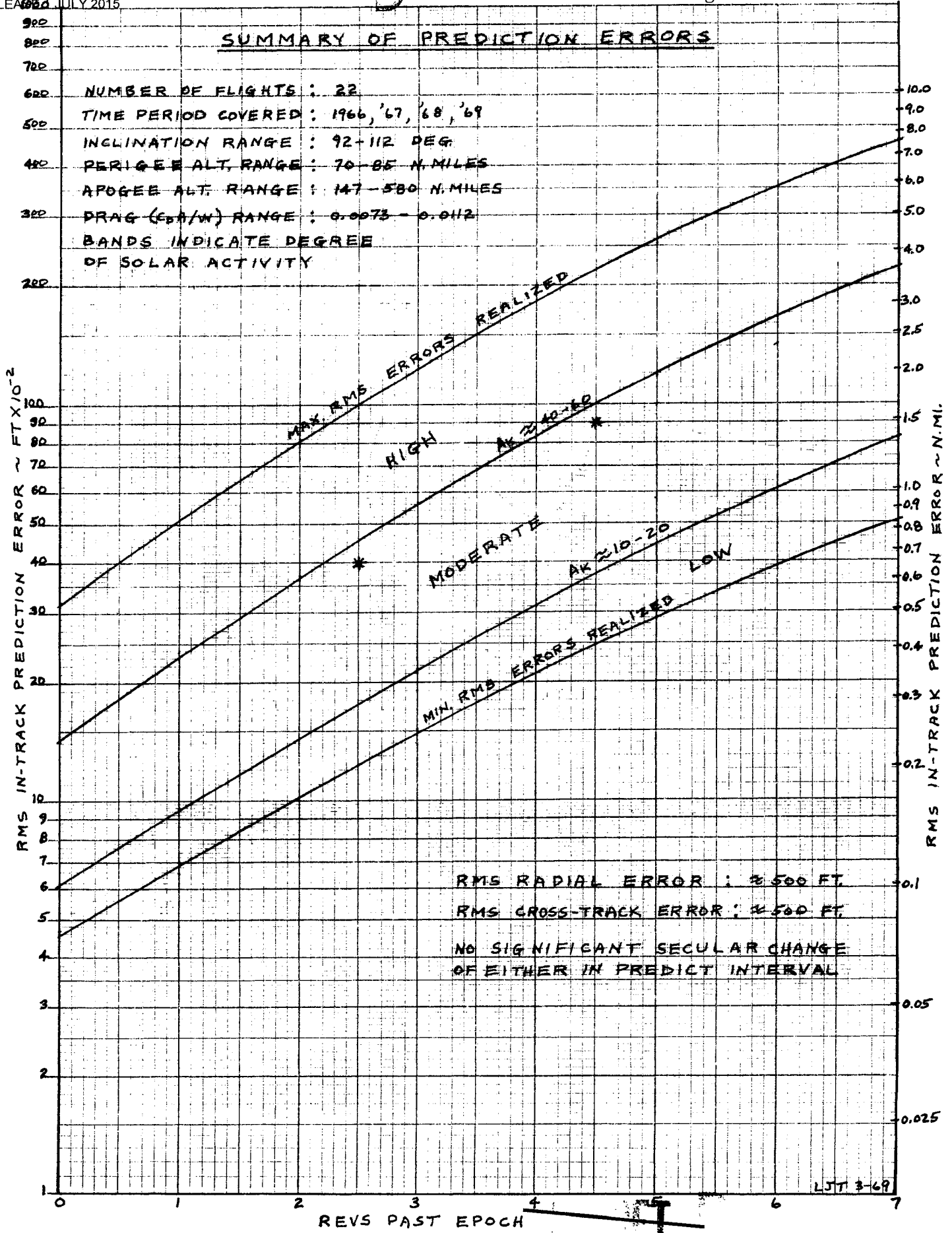
ANALYSIS OF IN-TRACK ERROR REDUCTION  
AT 4 1/2 REVS PAST EPOCH USING  
REPRESENTATIVE VALUES

$$2\sigma \Delta \text{In-Track} = \sqrt{(2\sigma)_{\text{Per}}^2 + (2\sigma)_{\text{Drag}}^2 + (2\sigma)_{\text{IC}}^2}$$

|  | <u>Total</u>  | <u>Period</u> | <u>Drag</u> | <u>IC</u>       |
|--|---------------|---------------|-------------|-----------------|
| W/O LGA/LRL<br>In Fit or Predict         | 18000         | 12600         | 12600       | 2500            |
| W LGA In Fit                             | 12650 - 12750 | 900           | 12600       | 400 - 1600      |
| W LGA In Fit<br>and Predict              | 1900 - 2450   | 900           | 1600        | 400 - 1600      |
| Above Plus Single LRL At                 |               |               |             |                 |
| E + 3                                    | 1000 - 1850   | 300           | 900         | 400 - 1600      |
| E + 4                                    | 550 - 1650    | 100           | 350         | 400 - 1600      |
| Above Plus LRL<br>Extrapolation at E and |               |               |             |                 |
| E + 3                                    | 1000 - 1850   | ≈ 0           | 900         | 400 - 1600      |
| E + 4                                    | 550 - 1650    | ≈ 0           | 350         | 400 - 1600      |
| Above Plus Geopotential<br>Improvement   |               |               |             |                 |
| E + 3                                    | 1000          | ≈ 0           | 900         | 400 } Objective |
| E + 4                                    | 500           | ≈ 0           | 350         | 400 }           |

~~SECRET~~ D

NRO APPROVED FOR  
RELEASE 1984 JULY 2015

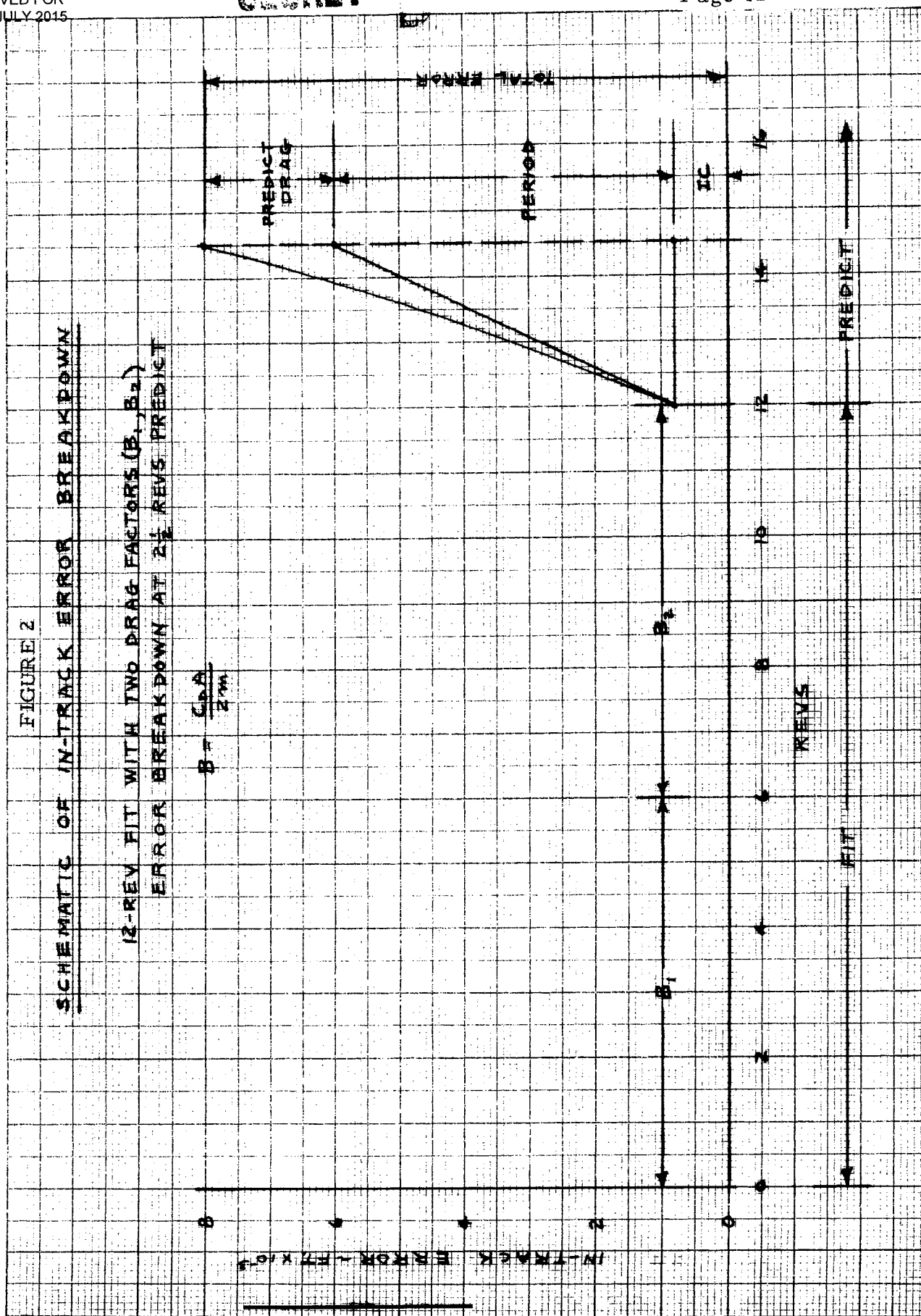


SEMI-LOGARITHMIC 46 5493  
REF ID: A66007

~~SECRET~~

FIGURE 2  
SCHEMATIC OF IN-TRACK ERROR BREAKDOWN  
12-REV HIT WITH TWO DRAG FACTORS ( $B_1, B_2$ )  
ERROR BREAKDOWN AT 2 1/2 REVS PREDICT

$$B = \frac{C_0 A}{2 \pi m}$$



~~SECRET~~

D

APPENDIX

Obtaining Error Estimates from Operational Data

The basic data used in constructing Figure 1 was generated at the Satellite Test Center, Sunnyvale, during actual flights. Tracking data obtained from the six-station SCF net was fit over 12-rev spans, on a least-square basis, to obtain vectors for command messages. Most of the fits solved for six orbit parameters and two drag factors ( $B_1$ ,  $B_2$ ) covering six revs each, while others solved for six orbit parameters and only one drag factor (covering 12 revs). Prediction characteristics from the two groups were close enough to allow the combining of data on one chart.

Operationally, after a fit has covered on a solution vector, the ascending node crossing system times are generated for all revs within the fit and eight revs beyond (prediction interval). The quality of the prediction is not determined until at least four subsequent fits include part or all of the prediction interval within their spans. The average of the node crossing time for a particular rev within the spans of these four fits then provides a reference for that same rev which is in the prediction interval of the earlier fit. The difference of these two node crossing times (predicted minus reference) then is the time-of-arrival difference at the ascending node, or a measure of the in-track error realized at that rev when predicting with parameters solved from the fit.

The in-track prediction errors from the many fits of the flights analyzed (about 12 fits per day, 5-10 days per flight) were first compiled on an RMS basis according to the degree of solar activity, and then plotted as in Figure 1. The ordinate for this initial plot was, however, the node crossing time error in seconds, and the rev index numbers on the abscissa were at the ascending nodes. As mentioned before, some flights were subdivided if marked differences in solar activity existed within each. In some cases, the rev 0 values had been obtained operationally, and in other cases these values were extrapolated from the revs 1-7 curves.

The last two steps in constructing Figure 1 from operational data involved, first, the converting of ascending node crossing time errors in seconds to position errors in feet. This was done by multiplying the ordinates of the original plot by a velocity at the ascending node typical of the orbits covered. This velocity was taken as 25,200 fps. The second step was to adjust the abscissa such that the rev indices denote revs past epoch instead of ascending nodes in the predict interval. The rev 0 index on the original abscissa was the ascending node of the epoch rev, and for command messages the epoch position is typically about 1/6 revs beyond this point. Therefore, to enable revs past epoch to be read directly from the final plot (Figure 1), the error curves were moved that amount to the left relative to the original indices.

~~SECRET~~

D